Mechanism of the silicon influence on chilling tendency index and chill of ductile iron in thin wall castings

In the present work an analytical expression that combines the susceptibility of liquid cast iron to solidify according to the Fe-C-X metastable system (also known as the chilling tendency of cast iron), is proposed. A relationship between the chilling tendency index of cast iron and several factors has been presented. The results can be also used as a guide for a better understanding of the effect of technological variables such as the melt chemistry, the holding time and temperature, the spheroidizing and inoculation practice, the resulting nodule count and the type of mold material and pouring temperature, on the resultant chill of the ductile iron. Theory was experimentally verified using silicon as an example. In particular, it has been shown that as a result of increasing silicon content the critical nodule count increases, and the temperature range between the graphite eutectic equilibrium temperature and formation temperature for cementite eutectic. Such variations lead to decreasing the chilling tendency index and in consequence reducing chills in cast iron. The chilling tendency index has been related to the critical wall thickness, below which the chill is formed. Theoretical calculations of the critical wall thickness were made and then compared with experimental outcome for ductile iron melts.

Edward Fraś, Krakow, Poland,
Jorge Antonio Sikora, Mar del Plata, Argentina,
and Marcin Górny, Krakow, Poland

Manuscript received 17 August 2009;
accepted 2 November 2009

E. Fraś, AGH – University of Science and Technology, Krakow, Poland, **J. A. Sikora**, National University of Mar del Plata, Mar del Plata, Argentina, **M. Górny**, AGH – University of Science and Technology, Krakow, Poland

1 Introduction

Significant efforts have been conducted recently towards the study of several aspects related to the production of thin wall ductile iron (TWDI) in order to introduce ductile iron pieces into the light parts market. As for all gray irons both, kinetic and thermodynamic factors influence the solidification structure and the final microstructure of TWDI. Very fast cooling rates, as those imposed during the solidification of TWDI parts, increase eutectic undercooling and may cause the formation of ledeburitic carbides, while slow cooling favors graphite precipitation. On the other hand, thermodynamic factors are related to the influence of alloying elements, particularly silicon. The susceptibility of the melt to solidify according to the Fe-C-X metastable system is known as the chilling tendency. In the foundry practice, the chilling tendency for the various types of cast irons is determined from comparisons of the exhibited fraction of cementite eutectic (chill) in castings solidified under similar cooling rate. **Figure 1** gives a comparison of the chilling tendency for two cast irons (I and II). Cast iron I exhibits a lower chilling tendency than cast iron II. Based only on these comparisons, the difference in the chilling tendency of various cast irons can be established.

In particular, cast irons possessing a high chilling tendency are prone to develop zones of white or mottled iron. Considering that these regions can be extremely hard; their machinability and mechanical properties can be severely impaired. Alternatively, if white iron is the desired structure a relatively small chilling tendency favors the formation of grey iron which in turn leads to poor hardness and wear properties for the cast components. Hence, considerable efforts have been made in correlating various factors of technological relevance, such as chemical composition [1-4], pouring temperature [2], spheroidization and inoculation practice [2, 3, 5, 6], casting geometry [7], plate thickness [2, 3, 7], mold material [8], and nodule count[1] with the chill of cast iron. These experimental relationships are very useful but they are limited in their physical meaning. Accordingly, in this work an analytical expressions is presented aiming to estimate quantitatively the chill formation. The main objective of this paper is to evaluate a new derived chilling tendency index of cast iron which can be theoretically calculated and related to of the critical wall thickness below which the chill is formed and verified by experiments.

2 Experimental procedure

TWDI plates, cast for a previous work [4] at the foundry pilot plant of the INTEMA Research Institute, have been used to validate the theoretical calculations. Three unalloyed ductile iron melts were produced by using a 55 kg capacity medium frequency induction furnace.

Charges were made using regular quality raw materials. The melts were superheated up to 1550 °C before tapping. Nodularization was carried out using the sandwich method and 1.5 % of Fe-Si-Mg (6 % Mg). They were inoculated with 0.6 % Fe-Si (5 % Si) in the stream. The melts had slight differences in carbon content and noticeable variations in silicon percentage, as it is indicated in **Table 1**. The plates were cast using a horizontal model. The moulds were made of resin bonded 60/62 sand and the inner surfaces were coated with graphite paint. Six plates of 120 × 40 mm

were obtained from each mould. Three of them had 1.5 mm thickness, while the others had 2, 3 and 6 mm thickness, respectively. **Figure 2** shows a casting which includes a fluidity spiral used to evaluate the castability.

As it can be seen all the plates, including the thinner ones were cast without significant cast defects. The microstructure of the samples was characterized on surfaces obtained by cutting the plates in the central zone. The microstructure characterization was aided by the use of the Image Pro Plus software. Nodule count was measured on unetched samples considering a nodule diameter threshold of 5 microns. In ductile iron the graphite nodules are characterized by Raleigh distributions [9] so the volumetric nodule count (nodule count per unit volume), N can be related to the planar nodule count (nodule count per unit area), N_F using the Wiencek equation [10]

$$N = \sqrt{\frac{N_F}{f_{gr}}} \tag{1}$$

where f_{gr} is the volume of graphite at room temperature, $f_{gr} \approx 0.11\text{-}0.14$.

The amount of carbides (area percentage) has been measured after etching with nital. Reported values of nodule count and carbide content are the average of at least five readings on each sample, at × 100 magnification. As an example, **Figure 3** shows the microstructure of a sample of 3 mm thickness corresponding to melt 1.

3 Analysis of results and discussion

By combining heat extraction and heat generated during solidification of spherical eutectic laws with kinetic growth laws and nodule count the solidification process of ductile iron has been calculated [11]. This analysis indicates that the critical wall thickness s_{cr} below which the chill is formed, can be given by

$$s_{cr} = 2\ p\ CT \tag{2}$$

where

$$p = a\left(\frac{T_s^3}{4\ \pi^5\ \beta\ B^2\ L_e^2\ z^2\ c^4}\right)^{1/6} \tag{3}$$

$$CT = \frac{1}{D^{1/2}}\left[\frac{1}{N_{v,cr}\ \beta\ \Delta T_{sc}^2}\right]^{1/3} \tag{4}$$

$$\Delta T_{sc} = T_s - T_c \tag{5}$$

$$B = \ln\frac{T_i}{T_s} \tag{6}$$

$$z = 0.41 + 0.93\ B \tag{7}$$

In the above equations: CT is the chilling tendency index of cast iron, T_i is the initial metal temperature just after filling the mould, $N_{v,cr}$ is the volumet-

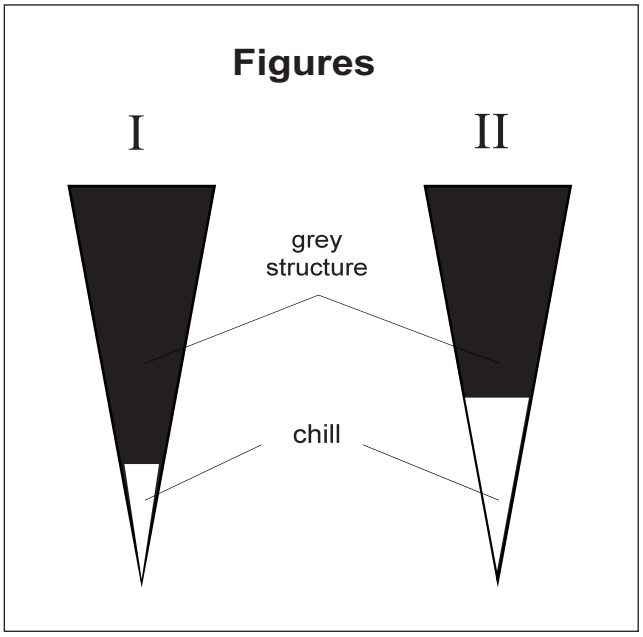

Figure 1: Castings according to ASTM standard for chill and chilling tendency estimation

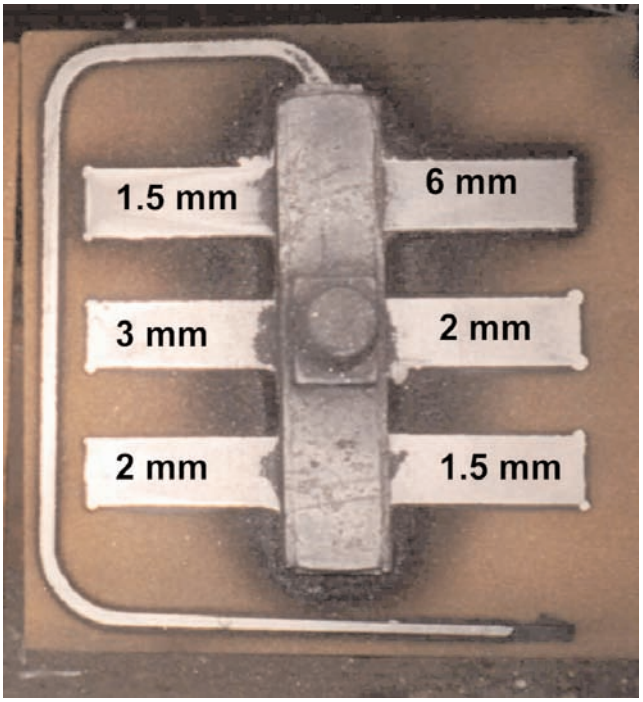

Figure 2: Casting showing the plates of different wall thicknesses

Table 1: Selected thermophysical data [11, 12]

Parameter	Value and units
Latent heat of graphite eutectic	L_e = 2028.8 J/cm^3
Specific heat of cast iron	c = 5.95 J/(cm^3 °C)
Material mould ability to absorb heat	a = 0.10 J/(cm^2 s$^{1/2}$ °C)
Formation temperature for cementite eutectic	T_c = 1130.56 + 4.06(C – 3.33 Si – 12.58 P) [°C]
Graphite eutectic equilibrium temperature	T_s = 1154.0 + 5.25 Si – 14.88 P [°C]

C, Si, P – content of carbon, silicon and phosphorus in cast iron, respectively, wt %

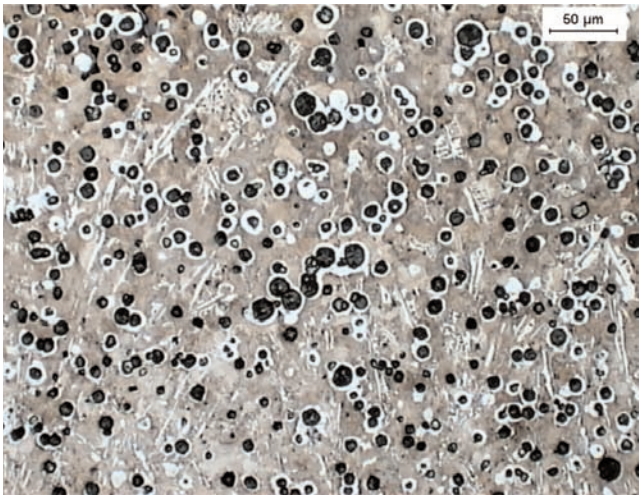

Figure 3: As cast microstructure of a 3 mm thickness sample of melt 1, containing 9 % carbides (etched with nital 2 %)

ric critical nodule count at temperature $T_m \approx T_c$ (when chill appears in the critical wall thickness s_{cr}, as shown in **Figure 4**b), D is the diffusion coefficient of carbon in austenite, and β is the coefficient (see Equation (15)). The terms L_e, c, a, T_c and T_s are defined in Table 1.

Table 2 shows results, for both, chemical composition and wall thickness, as well as the exhibited nodule count and cementite fraction of the melts used.

3.1 Chilling tendency index CT

From our experimental data and the theoretical perspective, the role of the silicon on the chilling tendency index CT of ductile iron can be disclosed based on Equation (4).

3.1.1 Influence of the temperature range $\Delta T_{sc} = T_s - T_c$

ΔT_{sc} (Figure 4a) range depends on the melt chemistry (Table 1). For the melts used (Table 2) the values of carbon and phosphosus content range from 3.31 to 3.45 and from 0.044 to 0.051 %, respectively. Taking into account average values C = 3.38 % and P = 0.047 %, ΔT_{sc} can be described by

$$\Delta T_{sc} = 11.3 + 18.8\ Si \qquad [°C] \qquad (8)$$

It can be observed that as Si contents increase, the ΔT_{sc} range also increases, and Equation (4) indicates that the chilling tendency index CT decreases.

3.1.2 Influence of the diffusion coefficient of carbon in austenite, D

This coefficient is related to solidification temperature of eutectic, T_m and chemical composition of the austenite. The effect of Si, Mn and P on D is not considered in this work, as there is not enough information available in the literature. An expression for the diffusion coefficient of carbon in austenite has been taken from the literature [13] which is given by:

$$D = \left(0.00453 + \frac{3.33957}{273.3 + T_m}\right) \exp \left(3.37065 - \frac{15176.273}{273.3 + T_m}\right) \qquad [cm^2/s] \qquad (9)$$

where T_m is the eutectic solidification temperature [°C].

The change of silicon content from 2.70 to 4.42 % (see Tables 1 and 2) can modify theoretically the eutectic solidification temperature, T_m during the eutectic transformation from $T_m = T_s = 1176$ °C to $T_m = T_c = 1084$ °C. So, for these values of T_m the D values in accordance with Equation (9) range from 2.7×10^{-6} to 5.6×10^{-6} cm²/s. Therefore, as Si content increases, D can decreases, and from Equation (4) result that the chilling tendency index increases.

3.1.3 Influence of the critical nodule count

The critical nodule count is represented by N_{cr} in Figure 4b. It is well known that each graphite nucleus gives rise to a single nodule, so it can be assumed that the measure of

Table 2: Chemical composition, wall thicknesses, nodule count, cementite fraction and chilling tendency index CT

Melt no	C, wt %	Si wt %	P, wt %	Wall thickness, mm experimental s	Wall thickness, mm calculated s_{cr}	Nodule count NF, mm^{-2}	Fraction of cementite, %	Chilling tendency, CT, $s^{1/2}/°C^{1/3}$
I	3.40	2.70	0.046	6.0		588	0	0.68
				3.0		1039	9.0	-
				2.0	2.9-4.2	1380	24.0	-
				1.5		1311	34.0	-
II	3.45	2.91	0.044	6.0		854	0	0.60
				3.0	2.6-3.6	1037	7.3	-
				2.0		1100	24	-
III	3.31	4.42	0.051	6.0		1127	0	-
				3.0		1726	0	-
				2.0	1.5-2.1	1890	0	0.34
				1.5		2027	9.3	-

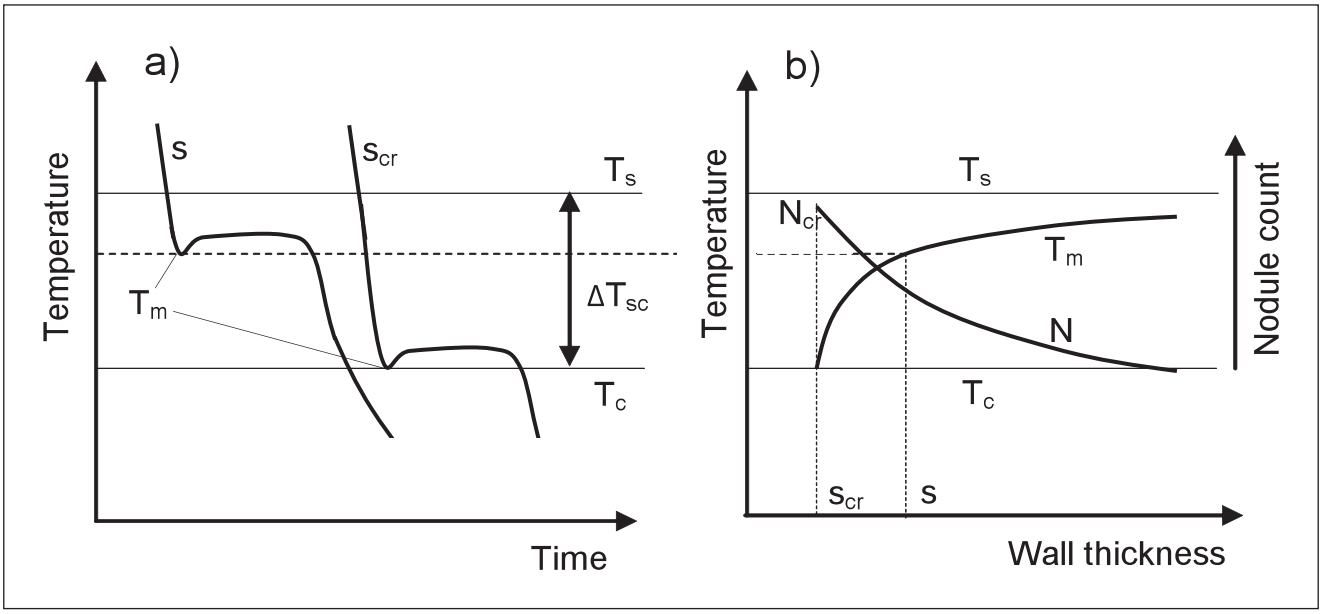

Figure 4: a) Cooling curves and b) effect of the wall thickness on the minimal eutectic solidification temperature, T_m and nodule count N; N_{cr} and s_{cr} are the critical nodule count and the critical wall thickness

graphite nuclei count, is the conventional nodule count. Accordance with Table 2, in melt I the transition from a wall thickness, s = 6 mm (without cementite) down to 3 mm (with cementite) is closely linked to a nodule count change from 588 to 1039 mm^{-2}. As a result, an average nodule count value of $N_{F,\,cr}$ = 813 mm^{-2} was used in this work. Similar determinations were made in melts II and III and $N_{F,\,cr}$ values of 945 and 1959 mm^{-2} has been obtained, respectively. **Figure 5** shows the relation between silicon content in cast iron and the critical nodule count, $N_{F,\,cr}$. This relationship can be described by

$$N_{F,\,cr} = 655.9\ Si - 982.9 \quad [mm^{-2}] \quad \text{or}$$
$$N_{v,\,cr} = 10^8\ (2.26 + 1.08\ Si) \quad [cm^{-3}] \qquad (10)$$

$N_{v,\,cr}$ is the volumetric critical nodule count.

Taking into account Equations (4) and (10) it can be concluded that as silicon content increases the $N_{F,\,cr}$ also increases and in consequence the chilling tendency index decreases.

3.1.4 Influence of the coefficient, β

From theoretical analysis of spherical eutectic growth [11] result the following equation

$$k = \frac{(C_3 - C_2)}{(C_4 - C_3)\left(\sqrt[3]{\frac{C_{gr} - C_2}{C_4 - C_3}} - 1\right)} \qquad (11)$$

where C_2, C_3, C_4 and C_{gr} are carbon content defined in **Figure 6**.

The above expression can be correlated with the degree of undercooling, ΔT. Assuming that the JE', E'S' and BC' lines for the Fe-C-Si system (Figure 6a) are straight the compositions in Equation (11) can be given by

$$C_2 = C_{E'} - 0.11\ Si - \frac{\Delta T}{m_2} \qquad (12)$$

$$C_3 = C_{E'} - 0.11\ Si + \frac{\Delta T}{m_3} \qquad (13)$$

$$C_4 = C_{C'} - 0.11\ Si - \frac{\Delta T}{m_4} \qquad (14)$$

where: m_2, m_3 and m_4 are the slopes of the line JE', E'S' and BC' respectively and $C_{E'}$, $C_{C'}$ are the carbon content in austenite and eutectic for Fe-C system, Si is the silicon content (wt %).

The following values can be employed [14]: $C_{C'}$ = 4.26 wt %, $C_{E'}$ = 2.08 wt %, m_2 = 275 [°C/wt %], m_3 = 189.6 [°C/wt %], and m_4 = 113.2 [°C/wt %]. Using this data, Equation (8) are plotted in **Figure 7**a. From this figure, it is apparent that k tends to

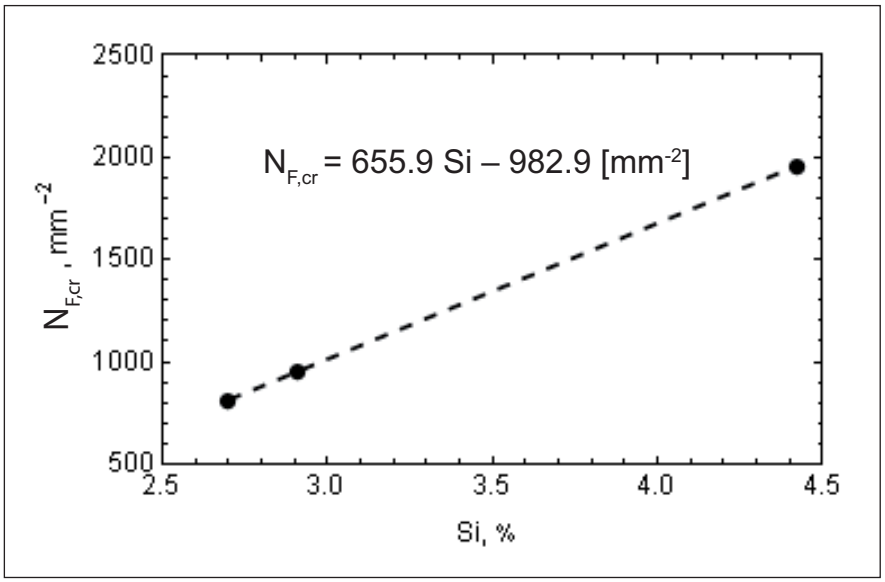

Figure 5: Correlation between silicon content in cast iron and critical nodule count, $N_{F,\,cr}$

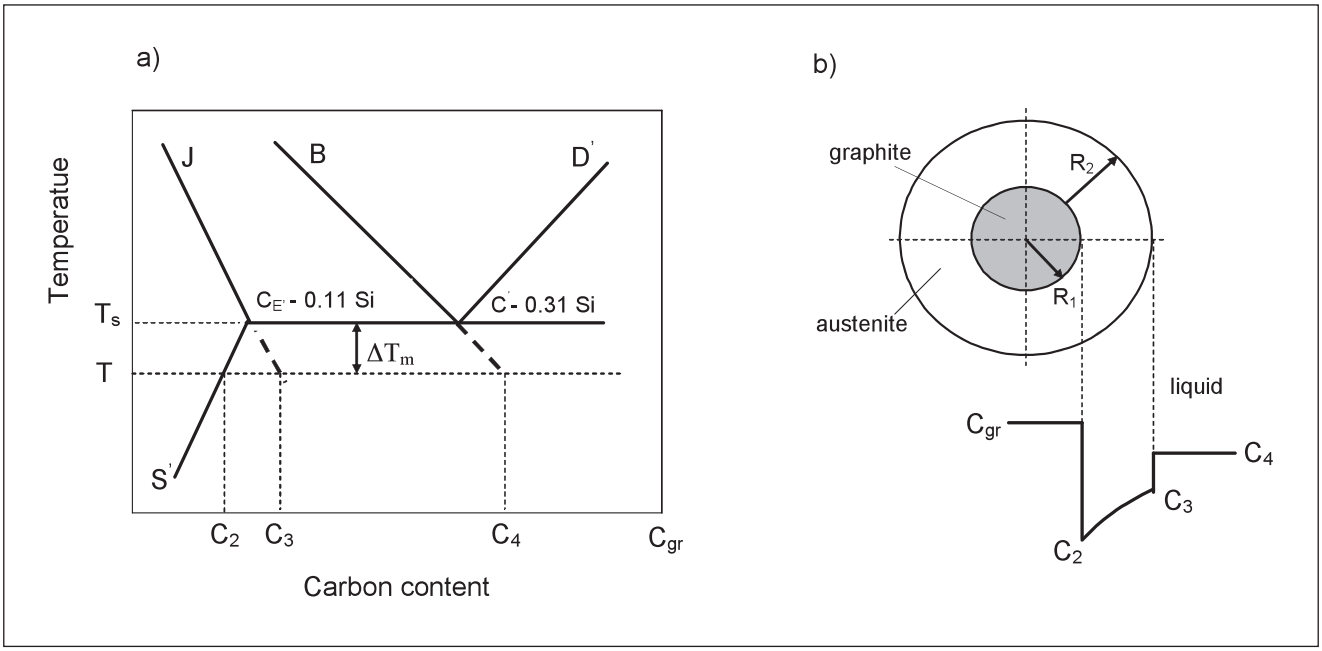

Figure 6: Schematic representation of a Fe-C-Si phase diagram (a) and corresponding carbon profile for a spherical eutectic cell (b)

exhibit a linear trend with ΔT. Accordingly, k can be described by

$$k = \beta \Delta T \quad (15)$$

where β are the slopes of the lines k(ΔT) in Figure 7a.

The effect of Si content on β values is given in Figure 7b. However, it can be shown by calculations that the effect of Si on s_{cr} and CT through β in Equations (15) and (4) is very small. Thus, it can be assumed that β is constant, β = 0,00155 °C^{-1}. This assumption gives the error about −3 % +6 % in our calculations.

All above parameters (N_v, $_{cr}$, ΔT_{sc}, D) depend on silicon content. So, the chilling tendency index can be presented as silicon function. For the calculation effect of silicon content on chilling tendency index, CT, the values of D ranging from 2.7×10^{-6} to 5.6×10^{-6} cm^2/s and Equations (4), (8) and (10) can be used. The results of these calculations are shown in **Figure 8**a. Thus, it can be stated that as silicon content increases the chilling tendency index of ductile iron decreases. It is quite well known that the chilling tendency determined by classic method of wedges decreases as silicon content increases. Thus, it can be stated that the present results reproduce the experimental knowledge.

3.2 Critical wall thickness s_{cr}

From Table 2, it is apparent that in melts I and II the chill occurs in walls with thicknesses between 3 and 6 mm,

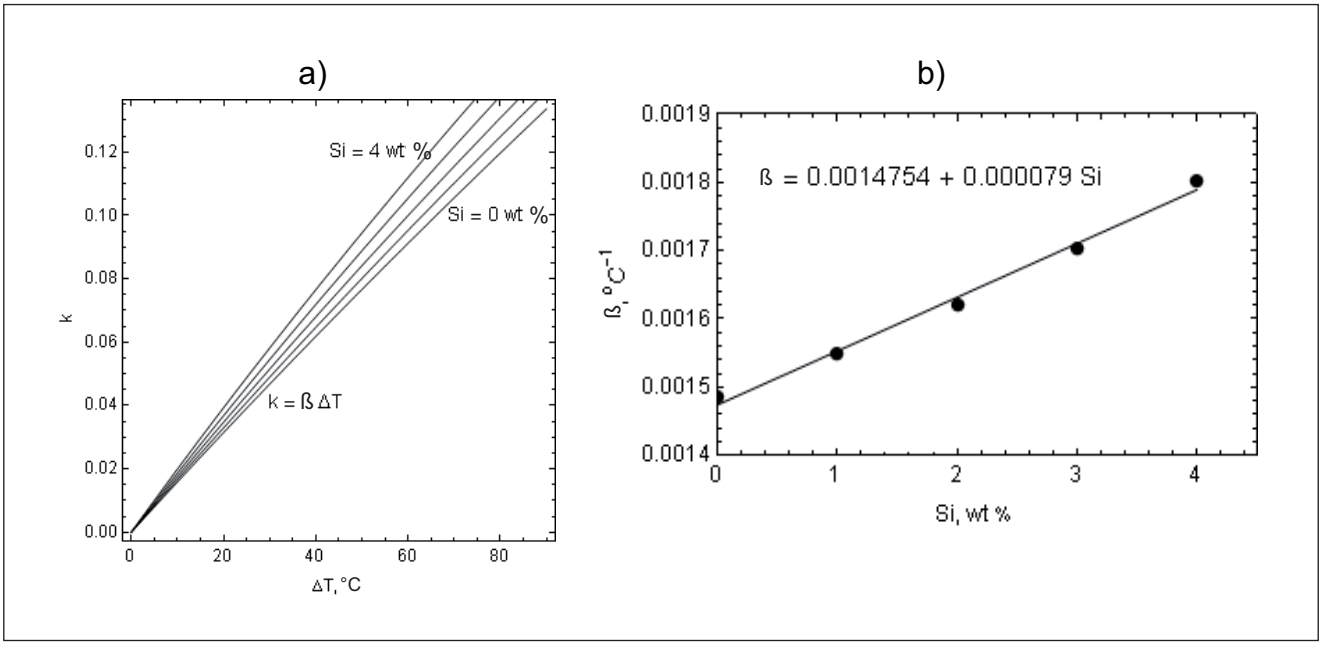

Figure 7: a) Plot of Equation (11) as function of the degree of undercooling and Si content and b) influence of Si content on the β values

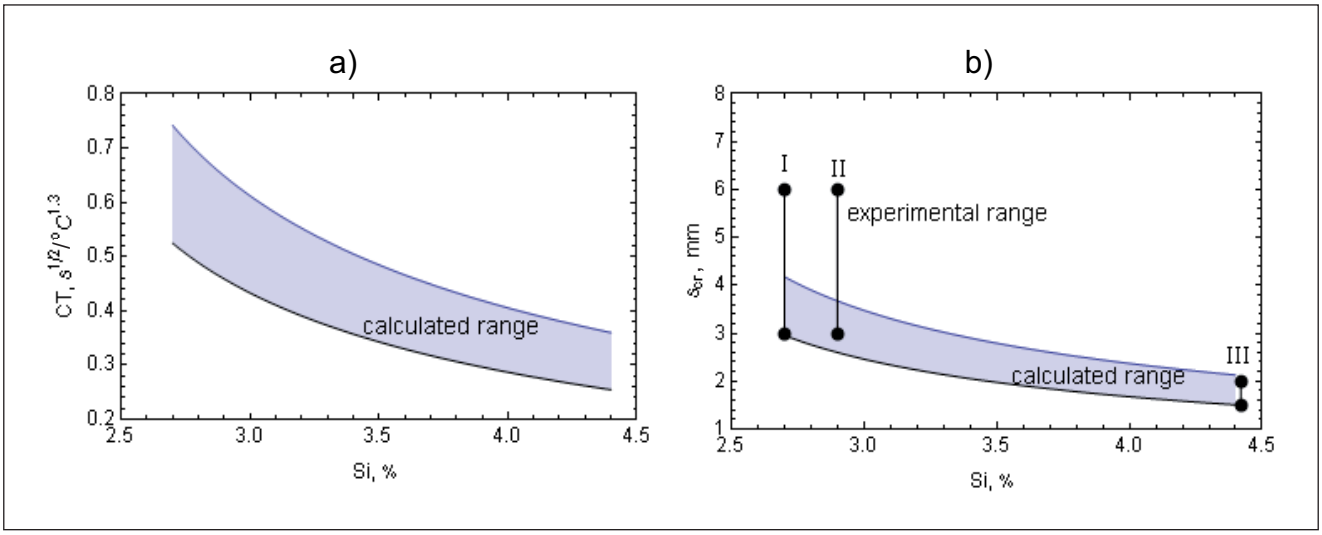

Figure 8: a) Influence of silicon content on chilling tendency index CT in cast iron and b) relation between silicon content and the critical wall thickness s_{cr} in ductile iron shadow area – calculated for D ranging from 2.7×10^{-6} to 5.6×10^{-6} cm²/s

while in melt III it happens at wall thicknesses between 1.5 and 2 mm. Hence, in order to compare these results with the theoretical predictions, estimations of s_{cr} were made, using Equation (2). In these calculations it was assumed that D = $2.7 \times 10^{-6} - 5.6 \times 10^{-6}$ cm²/s, a = 0.11 J/(cm² s $^{1/2}$ °C) and T_i = 1250 °C, other relevant information was taken from Table 1. Results of these calculations are shown in Figure 8b. From this figure, it can be observed that as Si contents increase from 2.70 to 4.42 %, the critical wall thickness, s_{cr} decreases from 2.9-4.2 to 1.5-2.1 mm. In addition, a comparison calculated s_{cr} indicates that the predictions from the theoretical analysis are rather in good agreement with the experimental data.

4 Conclusions

A simple theoretical analysis which enables the prediction of the chilling tendency index and chill in ductile cast iron has been presented. Theory was experimentally verified using silicon as an example. In particular, it has been shown that as a result of increasing silicon content nodule count, N and the critical nodule count, N_{cr} as well as the temperature range, ΔT_{sc} increases. Such variations lead decreasing the chilling tendency index, CT and in consequence reducing chills in cast iron. The chilling tendency index, CT has been related to the critical wall thickness, s_{cr} below which the chill is formed. Theoretical calculations of s_{cr} were made and then compared with experimental outcome for ductile iron melts.

The predictions of the theoretical analysis are in rather good agreement with the experimental data. Presented model is general and a real challenge would have been to apply this approach to predict chill tendency index in Fe-C-Ni or Fe-C-Cu systems.

Literature

[1] Javaid, A.; Thompson, J.; Davis, K. G.: Critical conditions for obtaining carbide-free microstructures in thin-wall ductile irons. AFS Transactions 110 (2002), pp. 889-898.
[2] Javaid, A.; Thompson, J.; Sahoo, M.; Davis, K. G.: Factors affecting the formation of carbides in thin-wall die castings. AFS Transactions 107 (1999), pp. 441-456.
[3] Ruxanda, R. E.; Stefanescu, D. M.; Piwonka, T. S.: Microstructure characterization of ductile thin-wall iron castings. AFS Transactions 110 (2002), pp. 1131-1148.
[4] Giacopini, A.; Boeri, R. E.; Sikora, J. A.: Carbide dissolution in thin wall ductile iron. Materials Science and Technology 19 (2003) no.12, pp. 1755-1760.
[5] Labrecque, C.; Gagne, M.: Production and properties of thin-wall ductile iron castings. International Journal of Cast Metal Research 16 (2003), pp. 313-317.
[6] Choi, J. H.; Oh, J. K.; Cho, C. O.; Kim, J. K.; Rohatgi, P. K.: Effect of Bi on formation of microstructure and mechanical properties of ductile iron castings with thin-wall section. AFS Transactions 112 (2004), pp. 831-840.
[7] Mampaey, F.; Xu, Z. A.: Mold filling and solidification of thin-wall ductile iron casting. AFS Transactions 105 (1997), pp. 95-103.
[8] Showman, R. E.; Aufderheide, R. C.: Process for thin-wall sand castings. AFS Transactions 111 (2003), pp. 567-578.
[9] Wojnar, R.: Effect of graphite size and distribution on fracture and fractography of ferritic nodular cast iron. Acta Stereologica 5 (1986), pp. 319-324.
[10] Wiencek, K.; Ryś, J.: The estimation of Fe_3C particle density in steel by simple counting measurements made in plane sections. Materials Engineering 17 (1986), pp. 396-399.
[11] Fraś, E.; Górny, M.; López, H.: Eutectic transformation in ductile cast iron. Part I, Theoretical background. Metallurgy and Foundry Engineering 31 (2005) pp.113-136.
[12] Fredriksson, H.; Svensson, I.: Computer simulation of the structure formed during solidification of grey cast iron, the physical metallurgy of cast iron. Editors: Fredriksson, H.; Hillert, M. North-Holland, New York 1985. Pp. 273-284.
[13] Agren, J.: A revised expression for the diffusivity of carbon in binary Fe-C austenite. Scripta Metallurgica 20 (1986), pp. 1507-1510.
[14] Metals Handbook, 8th edition, vol. 8. Metallography, Structures and Phase Diagrams. American Society for Metals, Metals Park, Ohio 1973. Pp. 275-278.